Numerical Study of Droplet Formation inside a Microfluidic Flow-Focusing Device

Yuehao Li, Mranal Jain and Krishnaswamy Nandakumar*
Cain Department of Chemical Engineering, Louisiana State University
*Corresponding author: 110 Chem. Eng. Bldg., LSU, Baton Rouge, LA, 70803, nandakumar@lsu.edu

Abstract:

Microfluidic flow-focusing (MFF) devices have been utilized for liquid-liquid emulsification processes because of its superior control. The micro-nanometer sized droplets have tremendous applications in bio-diagnostics, polymerization processes etc. In this work, we numerically investigate the droplet formation process of silicone oil in aqueous solution in a MFF device. A conservative level-set method is adopted to numerically model the droplet formation process numerically. The mono-dispersed and poly-dispersed droplet breaking processes are studied at different viscosity of the dispersed phase for a range of capillary number. The numerical solutions demonstrate good agreement with the experimental observations reported by Nie and co-workers for droplet size and poly-dispersity data. The interplay between the surface tension forces and shear forces at the interface governs the droplet size distribution during the breakup process. The poly-dispersed breaking is also influenced by the viscosity of the dispersed phase. This work may provide insight for the applications like emulsification, polymerization etc. where droplet size distribution is critical.

Keywords:
Droplet-based microfluidics, Level-set method, Flow-focusing

1. Introduction

Droplet-based microfluidics has been applied to synthesize polymer particles with various size, shapes and morphologies due to their sophisticated control on the polymerization process [1,2]. The droplet generating devices can be classified into three types: co-flow devices, cross-flow (T-junctions) devices, and flow-focusing devices [3]. Microfluidic flow-focusing (MFF) devices can generate droplets comparable to the size of the orifice; therefore, it is one of the most studied microfluidic mode of droplet breakup.

The droplet formation processes are affected by several parameters, i.e., flow rates, viscosity, dimensions of the geometry. Several researchers have carried out experimental studies on the droplet-breaking process in MFF devices [4,5,6]. The droplet breaking mechanisms are classified as squeezing, dripping and jetting regimes. The droplet breaking process is still not fully understood due to its dependence on large number of independent parameters such as flow rates, viscosities and geometric parameters.

Computational fluid dynamics (CFD) simulations provide an alternative approach to obtain insights into this complicated process. Typically, volume of fluid (VOF) method, level-set method (LS), phase-filed method, and lattice-Boltzmann method [7] are employed for modeling two phase flow. VOF method advects the volume fraction equation and adopts geometric construction to determine the weighted density and viscosity in each computational cell. Although VOF inherently conserves the mass, the interface is not accurately capture which results in leads to inaccuracy in estimated interfacial forces. For MFF devices with narrow orifice, the inaccurately captured thin interface might lead to large error if the droplet-breakup modeling is carried out using VOF. On the other hand, LS method represents the interface by a smooth function, and it is very convenient for calculation of curvature and surface tension forces. Therefore it appears more suitable for modeling droplet breaking process inside MFF devices.

In this study, we employ LS method to study the droplet-breaking process inside a M FF device. Silicone oil of various viscosities (10 cp, 20 cp, 50 cp and 100 cp) is used as the dispersed phase, and water is used as the continuous phase. The effects of capillary number (Ca) and viscosity of the dispersed phase (μ_d) on droplet-breaking process are investigated. The numerical results are benchmarked with the experimental study reported by Nie and co-workers [5].

Excerpt from the Proceedings of the 2012 COMSOL Conference in Boston

2. Numerical Method

In this work, the conservative level-set method that developed by Olsson and Kreiss [8] is adopted to simulate the droplet formation process. The conservative form of level-set method addresses the inherent mass-conservation problem of the classical LS method. The level-set equation is expressed as

$$\frac{\partial \phi}{\partial t} + \vec{u} \cdot \nabla \phi = \gamma \nabla \cdot \left(\epsilon \nabla \phi - \phi(1-\phi) \frac{\nabla \phi}{|\nabla \phi|} \right) \quad (1)$$

where the level-set function ϕ is in the range of 0 to 1. If $\phi < 0.5$, then it corresponds to phase 1; whereas $\phi > 0.5$, corresponds to phase 2; γ and ε are the stabilization parameters: ε determines the thickness of the interface where ϕ goes smoothly from 0 t o 1, and it should have the same order as the computational mesh size of the elements where interface propagates. The parameter γ determines the amount of reinitialization of the level set function. A suitable value for γ is the maximum value of the velocity field of $\vec{u}$.

The interfacial variables, the unit normal to the interface $\hat{n}$ and the curvature κ, then can be calculated by Eq. (2) and Eq. (3) respectively.

$$\hat{n} = \frac{\nabla \phi}{|\nabla \phi|} \quad (2)$$

$$\kappa = -\nabla \cdot \hat{n}|_{\phi=0.5} \quad (3)$$

The surface tension force acting on the interface between the two fluids is

$$\vec{F}_{sf} = \sigma \kappa \delta \hat{n} \quad (4)$$

where σ is the interfacial tension coefficient (N/m), κ is the curvature calculated from Eq. (3). δ is a Dirac delta function concentrated to the interface. The δ function is approximated by a smooth function according to

$$\delta = 6|\nabla \phi||\phi(1-\phi)| \quad (5)$$

The density ρ and viscosity μ in Eq. (1) are smoothed by ϕ across the interface.

$$\rho = \rho_1 + (\rho_2 - \rho_1)\phi \quad (6)$$

$$\mu = \mu_1 + (\mu_2 - \mu_1)\phi \quad (7)$$

The governing equations consist of the continuity equation (8) and the incompressible Navier-Stokes equation (9).

$$\frac{\partial \rho}{\partial t} + \nabla \cdot (\rho \vec{u}) = 0 \quad (8)$$

$$\frac{\partial (\rho \vec{u})}{\partial t} + \nabla \cdot (\rho \vec{u}\vec{u}) = -\nabla P + \nabla \cdot [\mu(\nabla \vec{u} + \nabla \vec{u}^T)] + \vec{F} \quad (9)$$

where $\vec{F}$ is the volume body force. As the density difference between the two phases is small, gravitational force is neglected; therefore, $\vec{F}$ only consists of the interfacial tension force.

3. Use of Comsol Multiphysics

The Two-Phase flow, Level-set for the CFD module in Comsol Multiphysics 4.2 is used for the numerical simulations. The simulations are carried out in a two dimensional domain, and the geometric dimensions and the computational mesh used in simulations are shown in Figure 1. After performing grid dependence studies with different grid resolutions, a numerical grid with 15,934 elements is adopted. Silicone oil is injected from the center inlet while aqueous solution is injected from the side inlets. The solutions are modeled as incompressible Newtonian fluids and the fluid properties aretaken directly from the data provided by Nie et al. [5]. The channel walls are specified as wetted wall condition with a constant contact angle for all the cases.

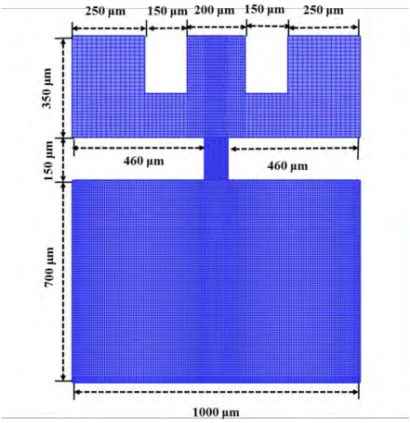

Figure 1 The geometry and mesh used in the numerical simulation

4. Results and Discussion

The results are discussed in terms of capillary number (Ca), $Ca = \frac{\mu_c u_c}{\sigma}$, based on the continuous phase, the flow ratio of the continuous phase to the dispersed phase (Q_o/Q_i) and the viscosity ratio of the dispersed phase to the continuous phase (μ_d/μ_c). At low Ca, the breaking mechanism is in the squeezing regime, also referred as "dripping regime–model 1" by Nie, where mono-dispersed droplets are produced in this regime. During the droplet formation process the dispersed phase blocks the entire orifice exit as shown in Figure 2(a), and mono-dispersed droplets are observed in this case.

Although the viscosity of the dispersed phase does not appear in the expression of Ca, it affects the breaking process. In Figure 2(b), the viscosity of the dispersed phase increases to 100 cp. Instead of blocking the entire orifice exit, the dispersed phase now forms a filament inside the orifice and a pendant droplet outside of the orifice.

Poly-dispersed droplets are observed in this case. Compared to the experimental observations, our numerical simulations can capture these two characteristics successfully as shown in Figure 2.

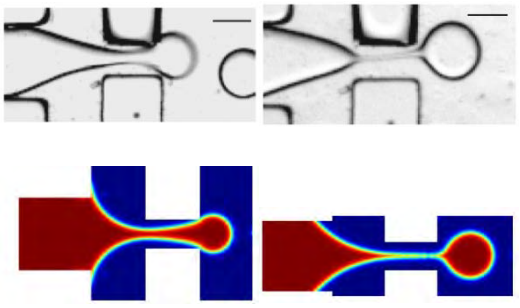

(a) (b)

Figure 2 Snapshots of droplet breaking process with different viscosities of the dispersed phase: (a) 20 cp (b) 100 cp. The flow rate of the dispersed phase is 0.04 mL/h, and the flow ratio (Q_o/Q_i) is 20. The upper pictures are the snapshots taken from the study by Nie et al. [5], and the lower ones are from numerical simulations.

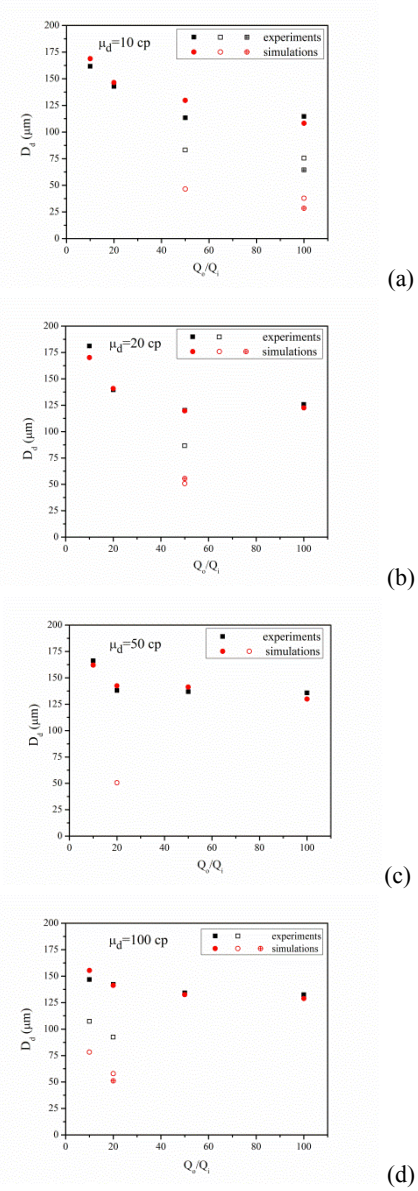

Figure 3 Droplet diameters as a function of flow ratios of continuous phase to dispersed phase. The flow rate of the dispersed phase for all the cases is 0.04 mL/h. The filled symbols correspond to the primary droplets while the open symbols correspond to the secondary droplets. If multiple secondary droplets are observed, only two are plotted to show the size range.

Figure 3 shows the quantitative agreement between the experiments and numerical simulation at various flow ratios and dispersed phase viscosities. The numerically estimated primary droplet sizes matches well with the

experimental data which suggests accurate modeling of the droplet breaking mechanisms.

Droplet formation exhibits three different modes based on the magnitude of Ca. At low Ca where viscous force is small, the droplet breaking process is dominated by squeezing regime, and mono-dispersed droplets are generated as shown in Figure 4.

As the dispersed phase propagates to the entrance of the orifice with a parabolic shape, it blocks the channel of the continuous phase thus builds up a high pressure upstream (Figure 4(a)). This high pressure squeezes the dispersed phase into the expanding channel (Figure 4(b)) and forms a visible neck inside the orifice (Figure 4(c)). Due to the high pressure and viscous stress exerted by the continuous phase, the neck collapses and a droplet larger than the orifice is separated from the dispersed phase (Figure 4(d)). The surface tension retracts the interface outside the orifice and same cycle is repeated.

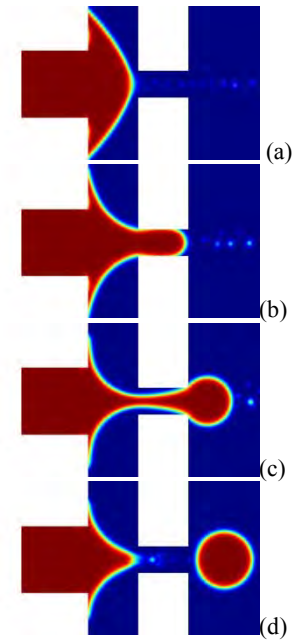

Figure 4 Droplet formation process at μ_d=20 cp and Q_o/Q_i = 10 where mono-dispersed droplets that are larger than the width of the orifice are observed in this case. The flow rate of the dispersed phase is 0.04 mL/h, and the corresponding Ca is 0.006.

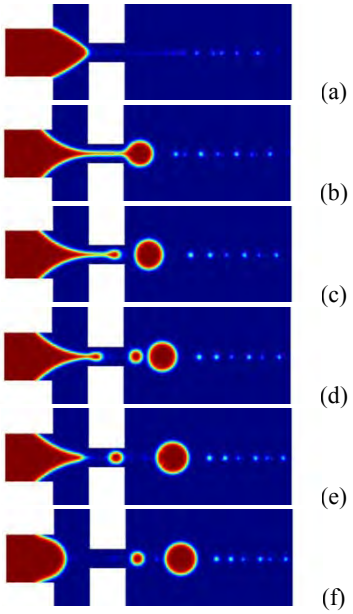

Figure 5 Droplet formation process at μ_d=20 cp and Q_o/Q_i = 50 where poly-dispersed breaking are observed in this case. The flow rate of the dispersed phase is 0.04 mL/h, and the corresponding Ca is 0.03.

Next Figure 5 shows a poly-dispersed breaking procedure at μ_d=20 cp and Q_o/Q_i = 50. When the interface propagates to the orifice entrance, it form a cone shape (Figure 5 (a)). Rather than blocking the entire orifice, the dispersed phase partially blocks the orifice and its exit (Figure 5 (b)). A thin thread is formed inside the orifice (Figure 5 (b)), and due to the viscous stress and pressure exerted by the continuous phase, a primary droplet breaks up from the thread (Figure 5(c)). The larger viscous shear force overcome the surface tension force that tend to retract the interface, thus the dispersed phase continues growing inside the orifice (Figure 5 (c)). A secondary droplet that is smaller than the orifice width is pinched off from the thread (Figure 5(d)). Due to its smaller size, this droplet is exerted by a smaller viscous resistance thus it catches up with the primary droplet and merges together (Figure 5 (d) and (e)). Meanwhile the thread is growing inside the orifice and forms another secondary droplet. The second satellite droplet is pinched off from the dispersed phase close to the entrance of the orifice (Figure 5 (e)). As the dispersed phase inside the orifice has been pinched off entirely, the surface tension force dominates the shear

force, thus the interface retracts back and a new sequence starts (Figure 5 (f)).

As Ca further increases, mono-dispersed breaking process occurs again. When the dispersed phase reaches the orifice entrance, it forms a cone-shape (Figure 6(a)). Due to the large flow rate of the continuous phase, the dispersed phase cannot block the orifice effectively (Figure 6(b)). A thin neck is formed inside the orifice. The tip of the orifice entrance cannot maintain a spherical shape because of the large shear force exerted by the dispersed phase (Figure 6(c)). Due to the existence of capillary wave instability [9], the strong shear stress creates wave shape on the neck (Figure 6(d)). The shear stress is sufficiently strong that the dispersed phase inside the orifice is pinched off from the dispersed phase and become tiny beads (Figure 6(e)). Compare to the primary droplet (D=122 μm), the diameter of the beads are much smaller (average diameter <10 μm) and cannot be captured accurately with LS method.

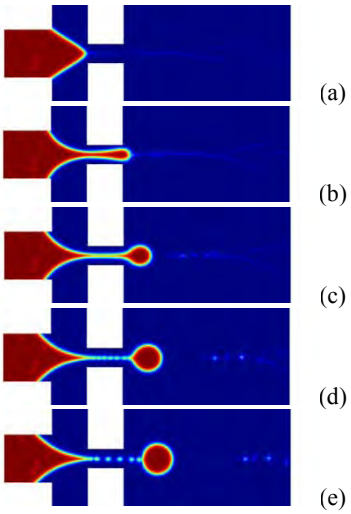

Figure 6 Droplet formation process at μ_d=20 cp and Q_o/Q_i =10 where monodispersed droplets are observed in this case. The flow rate of the dispersed phase is 0.04 mL/h, and the corresponding Ca is 0.06.

The viscosity of the dispersed phase also affects the dispersity of the droplets. Nie et al. [5] demonstrated the effect of dispersed phase viscosity on the droplet breakup process. Their study provides the droplet size and dispersity data for different values of the viscosity of the dispersed phase. Numerical simulations are performed with various viscosity values of the dispersed phase, and the results are shown in Figure 3. At low μ_d (μ_d=10 cp and 20 cp), poly-disperse occurs at relatively high Ca (Q_c/Q_d>50). As μ_d increases to 50 cp and 100 cp, poly-dispersed breaking occurs at low Ca (Q_c/Q_d=50). As μ_d increases to 500 cp, no poly-dispersed breaking is observed, which is not shown in this work.

The viscosity of the dispersed phase also influences the size of the droplets. As shown in Figure 3(a) and (b), increasing Ca can reduce the primary droplet sizes significantly for low μ_d. However, high μ_d in Figure (c) and (d) produces droplets of approximately same sizes for all the explored Ca. The droplet sizes from numerical simulations have good agreements with the experiemtal observations [5].

5. Conclusion and Future work

The droplet formation process in a MFF device has been captured numerically with the conservative LS method using Comsol Multiphysics. The presented results shows excellent qualitative and quantitive agreement with the experimental study [5]. We also investigated the different modes of droplet formation based on different capillary numbers. The obtained numerical results explains the reasons for the polydisperse droplet breakup. The effect of dispersed phase flow rate and the geometric dimensions on the droplet breaking processes will be analyzed in future work.

6. References

1. Nie, H., Xu, Q. S., Seo, M., Lewis, P. C., and Kumacheva, E., Polymer particles with various shapes and morphologies produced in continuous microfluidic reactors, *J. Am. Chem. Soc.*, **127**, 8058-8063, (2005).
2. Song, H., Chen, D. L. and Ismagilov, R. F., Reactions in droplets in microflulidic channels , *Angew. Chem.-Int. Edit.*, **45**, 7336-7356 (2006)
3. Christopher, G. F. and Anna, S. L., Microfluidic methods for generating continuous droplet streams, *J. Phys. D-Appl. Phys.*, **40**, R319-R336. (2007)
4. Lee, W., Walker, L. M. and Anna, S. L., Role of geometry and fluid properties in droplet and thread formation processes in planar flow focusing, *Phys. Fluids*, **21**, 032103 (2009)

5. Nie, Z. H., Seo, M. S., Xu, S. Q., Lewis, P. C., Mok, M., Kumacheva, E., Whitesides, G. M., Garstecki, P. and Stone, H. A., Emulsification in a microfluidic flow-focusing device: effect of the viscosities of the liquids, *Microfluid. Nanofluid.,* **5**, 585-594 (2008)
6. Garstecki, P., Stone, H. A. and Whitesides, G. M., Mechanism for flow-rate controlled breakup in confined geometries: A route to monodisperse emulsions, *Phys. Rev. Lett.,* **94**, (2005)
7. Liu, J. and Nguyen, N. T., Numerical Simulation of Droplet-Based Microfluidics - A Review, *Micro Nanosyst.*, **2**, 193-201 (2010)
8. Olsson, E., and Kreiss, G., A conservative level set method for two phase flow, *J. Comput. Phys.*, **210**, 225-246 (2005)
9. Zhou, C. F., Yue, P. T., Feng, J. J., Formation of simple and compound drops in microfluidic devices, *Phys. Fluids*, **18** (2006).

7. Acknowledgements

Authors would like to acknowledge the use of computing facilities of the Louisiana Optical Network Initiative (LONI) & High Performance Computing (HPC) facility at Louisiana State University and the continued funding from the Cain Chair program.